Title	Phase behavior of ethane hydrate system in the presence of ammonium bromide
Author(s)	Bando, Tatsuya; Sugahara, Takeshi
Citation	Fluid Phase Equilibria. 2016, 413, p. 36-40
Version Type	AM
URL	https://hdl.handle.net/11094/91304
rights	©2016. This manuscript version is made available under the CC-BY-NC-ND 4.0 license
Note	

Phase behavior of ethane hydrate system in the presence of ammonium bromide

Tatsuya Bando, Takeshi Sugahara[*]

Division of Chemical Engineering, Department of Materials Engineering Science, Graduate School of Engineering Science, Osaka University, 1-3 Machikaneyama, Toyonaka, Osaka 560-8531, Japan

[*] Corresponding author. Tel.: +81 6 6850 6293; fax: +81 6 6850 6293.

E-mail address: <u>sugahara@cheng.es.osaka-u.ac.jp.</u>

ABSTRACT

The three-phase equilibrium curves of hydrate, aqueous, and gas phases in the ternary system of ethane (C_2H_6), ammonium bromide (NH_4Br), and water were measured at pressures up to 3 MPa and temperatures of 278.45 to 283.76 K. The phase equilibrium curves exhibit two trends; the curve paralleled with that of simple C_2H_6 hydrate and the one steeper than that of simple C_2H_6 hydrate. The latter implies the incorporation of NH_4Br into C_2H_6 hydrate while the former indicates the thermodynamic inhibition effect of NH_4Br. To investigate the incorporation of NH_4Br, Raman spectra of the N–H stretching vibration of NH_4^+ were analyzed. Raman spectra imply the existence of the motionally restricted NH_4^+ in the formed hydrate. Both results from the phase behavior and Raman spectra imply the formation of $C_2H_6+NH_4Br$ semi-clathrate hydrates.

1. Introduction

Clathrate hydrate is an inclusion compound, which has an ice-like appearance. Guest species like light hydrocarbons and noble gases construct clathrate hydrates with host water molecules. There are several kinds of hydrate cages and a couple of them are combined to form specific hydrate structures. The structure-I (sI) hydrate consists of two 5^{12}-cages (pentagonal dodecahedron, hereafter called S-cages) and six $5^{12}6^2$-cages (M-cages) in the unit lattice. In the same manner, the structure-II (sII) hydrate is formed with sixteen S-cages and eight $5^{12}6^4$-cages (L-cages). Crystal structures and thermodynamic stabilities of gas hydrates mainly depend on the kind of guest species [1]. The familiar guest species for the sI hydrates are methane (CH_4), carbon dioxide (CO_2), ethane (C_2H_6). The CH_4 and CO_2 molecules are able to occupy both S- and M-cages [1-5]. The C_2H_6 molecule, whose molecular size is slightly larger than the void size of S-cage, occupies only the M-cages at pressures lower than approximately 20 MPa, while high pressures enable the occupancy of the C_2H_6 molecule in S-cages as well as M-cages [6].

Besides the regular clathrate hydrates, tetraalkyl ammonium or phosphonium salts with water form semi-clathrate hydrates [7-9]. Nitrogen or phosphorus atom as well as anions forms the hydrogen-bonded frameworks with water molecules. Shimada et al. [10] have reported the isobaric phase equilibrium (temperature–composition) relations for the tetra-*n*-butyl ammonium bromide (TBAB) semi-clathrate hydrate, one of the most famous substances forming semi-clathrate hydrates. The maximum equilibrium temperature of TBAB semi-clathrate hydrate at an atmospheric pressure with the TBAB aqueous solution (mass fraction of TBAB is 0.405) is 285.15 K.

Ammonia (NH_3) molecule, only from the viewpoint of molecular size, would be able to occupy the hydrate cages because its size is similar to that of CH_4. In fact, the previous studies [11-14] revealed that the water molecules form a dodecahedron cage (similar to S-cage) around NH_3 and ammonium ion (NH_4^+) in the gas phase. However, it had been believed that NH_3 does not form clathrate hydrates and behaves as a thermodynamic inhibitor to the clathrate hydrate formation [15,16]. Instead of clathrate hydrate formation, NH_3 hemihydrate ($2NH_3 \cdot H_2O$), NH_3 monohydrate

(NH$_3$·H$_2$O), and NH$_3$ dihydrate (NH$_3$·2H$_2$O) form at high pressures around 10 GPa (at room temperature) [17,18]. Shin et al. [19] reported the NH$_3$ clathrate hydrates (simple NH$_3$ hydrate, CH$_4$+NH$_3$ mixed hydrate, and tetrahydrofuran+NH$_3$ mixed hydrate) at low temperatures and the location of the NH$_3$ molecules in the hydrate crystal was estimated based on the results from molecular simulation.

In the present study, we have investigated whether ammonium salts, instead of the NH$_3$ molecule, are possible to be enclathrated under the coexistence of ethane (C$_2$H$_6$) as a hydrate former. The thermodynamic stability boundary of the clathrate hydrates formed in the ternary system of C$_2$H$_6$+ammonium bromide (NH$_4$Br)+H$_2$O was measured. Not only the possibility of the enclathration of NH$_4$$^+$ (also from the Raman spectra) but the effects of NH$_3$ and NH$_4$$^+$ on the thermodynamic stabilities were discussed.

2. Experimental

2.1. Apparatus

The pressure-proof glass cell (Taiatsu Techno, HPG-10-1) (inner volume: 10 cm^3, maximum working pressure: 5 MPa) was used for the phase equilibrium measurements. The experimental setup is the same as the one used previously [20,21]. The glass cell was immersed in the water bath where the temperature was controlled with the thermocontroller (Taitec, CL-80R). The equilibrium temperature was measured with the thermistor thermometer (Takara, D632, reproducibility: 0.02 K). The equilibrium pressure was measured with the pressure gauge (Valcom, VPRT, maximum uncertainty: 0.01 MPa).

2.2. Procedure

The NH$_4$Br (molar ratios of NH$_4$Br to H$_2$O are 1/35 (x_{NH4Br} = 0.028, w_{NH4Br} = 0.134) and 1/23 (x_{NH4Br} = 0.042, w_{NH4Br} = 0.191)) and NH$_3$ (molar ratios of NH$_3$ to H$_2$O are 1/35 (x_{NH3} = 0.028, w_{NH3} = 0.026), and 1/23 (x_{NH3} = 0.042, w_{NH3}= 0.040)) aqueous solutions were prepared with the

electric balance (Shimadzu BL-220H, maximum uncertainty is 0.004 g), where x and w stand for the mole fraction and mass fraction, respectively. A desired volume (each is approximately 2 cm^3) of NH_3 or NH_4Br aqueous solutions was introduced into the glass cell and degassed by a freezing method. The contents were pressurized with C_2H_6 up to a desired pressure. A magnetic stirrer was moved up and down by a permanent magnet outside for agitation of the gas-liquid interface as well as the contents. The up-and-down agitating is quite important for supplying a sufficient amount of C_2H_6 in to the aqueous solution through the gas–aqueous interface. The contents were cooled and agitated to generate mixed hydrates. After the hydrate formation, the system temperature was increased by 0.1 K step every 3 hours. When the disappearance of the last hydrate particle was confirmed, we determined that the system reached a three-phase equilibrium condition of H+L$_1$+G (H: hydrate phase, L$_1$: aqueous phase, G: gas phase) with a desired composition of NH_3 or NH_4Br in the aqueous solution. After the complete dissociation of the formed hydrates, the system temperature was increased by 0.1 K step every 3 hours. We confirmed the change of the slopes of the fitting curves before and after the complete dissociation.

For the Raman spectroscopy, the quenched NH_4Br aqueous solution (molar ratio of NH_4Br to H_2O was 1/35) was grained in the mortar immersed in liquid nitrogen. The powder with approximately 200 μm in diameter was loaded into the high-pressure cell and then pressurized up to 1.7 MPa with C_2H_6. The sample was prepared at temperatures of 267 K in a temperature-controlled chamber (ESPEC, SU-241) for a couple of days. Just 1 hour before the Raman analysis, the sample in the cell was moved to a cold room and kept at 253 K there. The pressure in the cell was then released and allowed to reach atmospheric pressure. Once released, the sample was kept at 77 K. A laser Raman microprobe spectrometer with a multichannel CCD detector (JASCO, NRS-1000) was used. The Diode Pumped Solid State (DPSS) laser (Cobolt, Fandango) was irradiated to the samples at atmospheric pressure and 77 K. The backscatter was taken in with same lens. The wavelength of the DPSS laser was 514.5 nm and the output power was adjusted to 100 mW. The spectral resolution of the obtained Raman spectra was approximately 1 cm^{-1}.

2.3. Materials

C$_2$H$_6$ (molar purity: 0.999) was purchased from Takachiho Trading Co., Ltd. Guaranteed research grade aqueous NH$_3$ solution with 28 mass%(NH$_3$) was obtained from Nakalai Tesque. NH$_4$Br (molar purity: 0.990) and distilled water were purchased from Wako Pure Chemical Industries, Ltd.   All materials were used without further purification.

3. Results and discussion

The three-phase equilibrium relations of the ternary system of C$_2$H$_6$+NH$_4$Br+H$_2$O were shown in Figure 1 and listed in Table 1.   As shown in Figure 1, two trends of phase behavior were observed in each NH$_4$Br mole fraction. One (closed circles and squares) is the curve (blue) paralleled with that of the simple C$_2$H$_6$ hydrate [22, 23], the other (open circles and squares) is the curve (red) steeper than that of the simple C$_2$H$_6$ hydrate in the pressure-temperature diagram.   The pressure and temperature relations of the simple C$_2$H$_6$ hydrate are correlated by the following equation:

$$\ln(p/p_0) = a + bT, \quad \text{where } p_0 = 1 \text{ MPa.} \qquad (1)$$

The above equation is superior to two-parameter Clausius-type equation.   The constants a and b in the simple C$_2$H$_6$ hydrate system are -38.504 and 0.13793 K^{-1} (the correlation coefficient r is 0.99787), respectively.   The blue curves were drawn with the same b value in eq. (1).   The drawn curves are fitted with the measured data.   The values a (and r) in the NH$_4$Br/water molar ratios of 1/35 and 1/23 are -38.106 (r = 0.93665) and -37.994 (r = 0.49159), where the r value is due to insufficient number of datum sets), respectively.

In the former (parallel and blue curves), NH$_4$Br plays a role as a thermodynamic inhibitor for sI simple C$_2$H$_6$ hydrate formation, because the parallel shift of three-phase equilibrium curve is one of the most characteristic features for the thermodynamic inhibition using salts [1,24,25].   Moreover, no Raman signal derived from NH$_4$Br was detected in the formed hydrates.   The latter (steeper and red curves) implies the possibility of the incorporation of NH$_4$Br to the clathrate hydrate.   When the

experimental datum sets (open squares) in the NH$_4$Br/water molar ratios of 1/35 are correlated with the eq. (1), the slope b was 0.22423 K^{-1} ($r = 0.99367$), which is larger than 0.13793 K^{-1} of the simple C$_2$H$_6$ hydrate system. Both steeper curves at the NH$_4$Br/water molar ratios of 1/35 and 1/23 have similar slope in the pressure-temperature projection. In the case of the molar ratio of 1/35, two curves intersect at 282.4±0.1 K and 2.31±0.04 MPa. Also in the case of the molar ratio of 1/23, the intersection would be located around 278.5±0.2 K and 1.8±0.1 MPa. The intersections are structural transition points. At temperatures higher than the points, the simple C$_2$H$_6$ hydrate phase is thermodynamically stable, while the C$_2$H$_6$+NH$_4$Br hydrate is under metastable state. The symbols (m) in Table 1 represent the data under metastable conditions. The data scatter in the system with the molar ratio 1/23 would be due to the metastability.

To investigate the incorporation of NH$_4$Br to the hydrate formation, Raman spectra for the hydrates prepared at a temperature below the structural transition point in the ternary system of C$_2$H$_6$+NH$_4$Br+water were measured. Raman spectra of the C–C stretching vibration of the C$_2$H$_6$ molecule are shown in Figure 2. The Raman peak in the C$_2$H$_6$+NH$_4$Br hydrate was detected at 994 cm^{-1}, while those in sI simple C$_2$H$_6$ hydrate and solid C$_2$H$_6$ were at 1000 cm^{-1} and 997 cm^{-1}, respectively. Raman spectra of N–H stretching vibration of NH$_4^+$ in the C$_2$H$_6$+NH$_4$Br hydrate are shown in Figures 3b and 4b. Figure 4 corresponds to the enlargement of 3200 to 3350 cm^{-1} in Figure 3. Figures 3 and 4 include the Raman spectra in the simple C$_2$H$_6$ hydrate (a), the solid NH$_4$Br powder (c), and the quenched NH$_4$Br aqueous solution (d). All samples were recorded at 77 K and 0.1 MPa. As shown in Figure 3, the intensive Raman peak was detected around 3040 cm^{-1}. In the solid NH$_4$Br powder (c) and the quenched NH$_4$Br aqueous solution (d), the peak was detected at 3036 cm^{-1}, which agrees with the N–H stretching vibration of NH$_4^+$ in pure crystalline NH$_4$Br [26]. In the C$_2$H$_6$+NH$_4$Br hydrate (b), the peak was detected at 3041 cm^{-1} that is 5 cm^{-1} different from the spectra (c) and (d). This Raman peak suggests the restricted NH$_4^+$ similar to that in the crystalline NH$_4$Br exists in the C$_2$H$_6$+NH$_4$Br hydrate, which implies that the C$_2$H$_6$+NH$_4$Br hydrate might be a semi-clathrate hydrate like TBAB semi-clathrate hydrate. The 2nd largest difference between the

spectra of (b) and others (a, c, and d) appears around 3275 cm^{-1}, as easily recognized in Figure 4. Only the spectrum in the C_2H_6+NH_4Br hydrate has the peak detected at 3275 cm^{-1}.   Price et al. [27] estimated that the N–H symmetric stretching vibration of free NH_4^+ should be detected at 3270±25 cm^{-1}.   The peak of 3275 cm^{-1} implies the existence of possible relatively-free NH_4^+ in the C_2H_6+NH_4Br hydrate.   There would be a possibility of an NH_4^+ enclathrated in a hydrate cage. Further investigation would be needed to clarify the location of NH_4^+ in the C_2H_6+NH_4Br hydrate.

The three-phase equilibrium curves of hydrates formed in the ternary system of C_2H_6+NH_3+water are listed in Table 2 and shown in Figure 5.   At both molar ratios of 1/35 and 1/23, the equilibrium curves are shifted to low-temperature and high-pressure side and almost paralleled with that of the simple C_2H_6 hydrate.   It means, under the present experimental temperature and pressure conditions, NH_3 plays a role as a thermodynamic inhibitor for the simple C_2H_6 hydrate formation, like for the simple CH_4 hydrate formation [15].   However, comparing its inhibition effect with that in C_2H_6+NH_4Br+water under the same molar concentration, the inhibition effect of NH_3 is quite smaller than that of NH_4Br.   One of the reasons why the difference occurs would be the different degrees of ionization between NH_4Br and NH_3 in their aqueous solutions. NH_4Br is completely ionized while the degree of ionization of NH_3 is 10^{-3} order even at 100 MPa [28].

4. Conclusions

The possible incorporation of NH_4Br into C_2H_6 hydrates has been investigated with the phase equilibrium measurement and Raman spectroscopy.   Two trends of phase behavior were observed in the ternary system of C_2H_6+NH_4Br+water.   One implies the formation of a C_2H_6+NH_4Br hydrate.   Raman spectra derived from NH_4^+ in the formed hydrate also imply it is a C_2H_6+NH_4Br semi-clathrate hydrate.   The other trend of phase behavior indicates the thermodynamic inhibition effect of NH_4Br on the simple C_2H_6 hydrate formation.   The structural transition point between the C_2H_6+NH_4Br semi-clathrate hydrate and the C_2H_6 hydrate inhibited with

NH$_4$Br is located at 282.4 K and 2.31 MPa with the NH$_4$Br/H$_2$O molar ratio of 1/35.   The inhibition effect of NH$_4$Br was much larger than that of NH$_3$ under the same mole fraction in the aqueous solution.   Under the present experimental condition, no NH$_3$ molecule occupies the hydrate cages.

List of symbols

p Pressure [Pa]

T Temperature [K]

x Mole fraction [-]

w Mass fraction [-]

$\Delta\nu$ Raman shift [cm^{-1}]

Acknowledgements

References

[1] E.D. Sloan, C.A. Koh, Clathrate Hydrates of Natural Gases, 3rd ed.; CRC Press, Taylor & Francis Group: Boca Raton, FL, 2008.

[2] A.K. Sum, R.C. Burruss, E.D. Sloan, Measurement of Clathrate Hydrates via Raman Spectroscopy. J. Phys. Chem. B 101 (1997) 7371–7377.

[3] S. Nakano, M. Moritoki, K. Ohgaki, High-Pressure Phase Equilibrium and Raman Microprobe Spectroscopic Studies on the Methane Hydrate System. J. Chem. Eng. Data 44 (1999) 254–257.

[4] F. Fleyfel, J.P. Devlin, Carbon Dioxide Clathrate Hydrate Epitaxial Growth: Spectroscopic Evidence for Formation of the Simple Type-II CO$_2$ Hydrate. J. Phys. Chem. 95 (1991) 3811–3815.

[5] P.S.R. Prasad, K. S. Prasad, N.K. Thakur, FTIR Signatures of Type-II Clathrates of Carbon

Dioxide in Natural Quartz Veins. Current Sci. 90 (2006) 1544–1547.

[6] K. Morita, S. Nakano, K. Ohgaki, Structure and Stability of Ethane Hydrate Crystal. Fluid Phase Equilibria 169 (2000) 167–175.

[7] D.L. Fowler, W.V. Loebenstein, D.B. Pall, C.A. Kraus, Some Unusual Hydrates of Quaternary Ammonium Salts. J. Am. Chem. Soc. 62 (1940) 1140–1142.

[8] Y.A. Dyadin, L.S. Zelenina, Y.M. Zelenin, I.I. Yakovlev, Clathrate Polyhydrates in Water-Tetra-*n*-butyl Phosphonium Bromide System. Izv. Sib. Otd. Akad. Nauk SSSR, Ser. Khim. Nauk 4, (1973) 30–33.

[9] L.S. Aladko, Y.A. Dyadin, T.V. Rodionova, I.S. Terekhova, Clathrate Hydrates of Tetrabutylammonium and Tetraisoamylammonium Halides. J. Struct. Chem. 43 (2002) 990–994.

[10] W. Shimada, T. Ebinuma, H. Oyama, Y. Kamata, S. Takeya, T. Uchida, J. Nagao, H. Narita, Separation of Gas Molecule Using Tetra-*n*-butyl ammonium Bromide Semi-Clathrate Hydrate Crystals. Japanese J. Appl. Phys. 42 (2003) 129–131.

[11] H. Shinohara, U. Nagashima, H. Tanaka, N. Nishi, Magic Numbers for Water-Ammonia Binary Clusters: Enhanced Stability of Ion Clathrate Structures. J. Chem. Phys. 83 (1985) 4183–4192.

[12] A. Khan, Theoretical Studies of $NH_4^+(H_2O)_{20}$ and $NH_3(H_2O)_{20}H^+$ Clusters. Chem. Phys. Lett. 338 (2001) 201–207.

[13] E.G. Diken, N.I. Hammer, M.A. Johnson, R.A. Christie, K.D. Jordan, Mid-infrared Characterization of the $NH_4^+ \cdot (H_2O)_n$ Clusters in the Neighborhood of the $n = 20$ "Magic" Number. J. Chem. Phys. 123 (2005) 164309-1–7.

[14] P.U. Andersson, M.J. Ryding, O. Sekiguchi, E. Uggerud, Isotope Exchange and Structural Rearrangements in Reactions between Size-Selected Ionic Water Clusters, $H_3O^+(H_2O)_n$ and $NH_4^+(H_2O)_n$, and D_2O. Phys. Chem. Chem. Phys. 10 (2008) 6127–6134.

[15] M. Choukroun, O. Grasset, G. Tobie, C. Sotin, Stability of Methane Clathrate Hydrates under Pressure: Influence on Outgassing Processes of Methane on Titan. Icarus 205 (2010) 581–593.

[16] T.H. Vu, E. Gloesener, M. Choukroun, A. Ibourichene, R. Hodyss, Experimental Study on the

Effect of Ammonia on the Phase Behavior of Tetrahydrofuran Clathrates. J. Phys. Chem. B 118 (2014) 13371–13377.

[17] J.I. Lunine, D.J. Stevenson, Clathrate and Ammonia Hydrates at High Pressure: Application to the Origin of Methane on Titan. Icarus 70 (1987) 61–77.

[18] A.D. Fortes, M. Choukroum, Phase Behaviour of Ices and Hydrates. Space Sci. Rev. 153 (2010) 185–218.

[19] K. Shin, R. Kumar, K.A. Udachin, S. Alavi, J.A. Ripmeester, Ammonia Clathrate Hydrates as New Solid Phases for Titan, Enceladus, and Other Planetary Systems. PNAS 109 (2012) 14785–14790.

[20] N. Shimada, K. Sugahara, T. Sugahara, K. Ohgaki, Phase Transition from Structure-H to structure-I in the Methylcyclohexane+Xenon Hydrate System. Fluid Phase Equilib. 205 (2003) 17−23.

[21] K. Sugahara, M. Yoshida, T. Sugahara, K. Ohgaki, Thermodynamic and Raman Spectroscopic Studies on Pressure-Induced Structural Transition of SF_6 Hydrate. J. Chem. Eng. Data 51 (2006) 301 − 304.

[22] O.L. Roberts, E.R. Brownscombe, L.S. Howe, H. Ramser, Constitution Diagrams and Composition of Methane and Ethane Hydrates, Oil and Gas Journal 39 (1940) 37 − 43.

[23] W.M. Deaton, E.M. Frost, Jr., Gas Hydrates and Their Relation to the Operation of Natural-Gas Pipe Lines, U.S. Bureau of Mines Monograph 8, p. 101, 1946.

[24] R. Kobayashi, H.J. Withrow, G.B. Williams, D.L. Katz, Gas Hydrate Formation with Brine and Ethanol Solutions. Proc. 30th. Ann. Convention Natural Gasoline Association of America 1951 (1951) 27 − 31.

[25] J.L. de Roo, C.J. Peters, R.N. Lichtenthaler, G.A.M. Diepen, Occurrence of Methane Hydrate in Saturated and Unsaturated Solutions of Sodium Chloride and Water in Dependence of Temperature

and Pressure. AIChE J. 29 (1983) 651 − 657.

[26] Y. Yamaguchi, H.F. Schaefer III, A Systematic Theoretical Study of Harmonic Vibrational Frequencies: The Ammonium Ion NH_4^+ and Other Simple Molecules. J. Chem. Phys. 73 (1980) 2310 − 2318.

[27] J.M. Price, M.W. Crofton, Y.T. Lee, Vibrational Spectroscopy of the Ammoniated Ammonium Ions $NH_4^+(NH_3)_n$ (n = 1-10), J. Phys. Chem. 95 (1991) 2182 − 2195.

[28] J. Buchanan, S.D. Haman, The Chemical Effects of Pressure, Transactions of the Faraday Society 49 (1953) 1425 − 1433.

Figure caption

Fig. 1.   Three-phase equilibrium curves of hydrate+aqueous+gas phases in the ternary system of C_2H_6+NH_4Br+water and the binary system of C_2H_6+water [22,23].

Fig. 2.   Raman spectra of the C–C stretching vibration of C_2H_6 molecule in the simple C_2H_6 hydrate (a), NH_4Br+C_2H_6 hydrate (b), and solid C_2H_6 (c).   All spectra were recorded at 77 K and 0.1 MPa.

Fig. 3.   Raman spectra of the N–H stretching vibration of NH_4^+ in NH_4Br+C_2H_6 hydrate (b), powder NH_4Br (c), and quenched NH_4Br aqueous solution (d).   The spectrum (a) corresponds to the O–H vibration region in the simple C_2H_6 hydrate.   All spectra were recorded at 77 K and 0.1 MPa.

Fig. 4.   Enlargement around 3280 cm^{-1} in Figure 3.

Fig. 5.   Three-phase equilibrium curves of C_2H_6 hydrate+aqueous+gas phases in the ternary

systems of C_2H_6+NH_3+water (green curves) and C_2H_6+NH_4Br+water (blue curves) and the binary

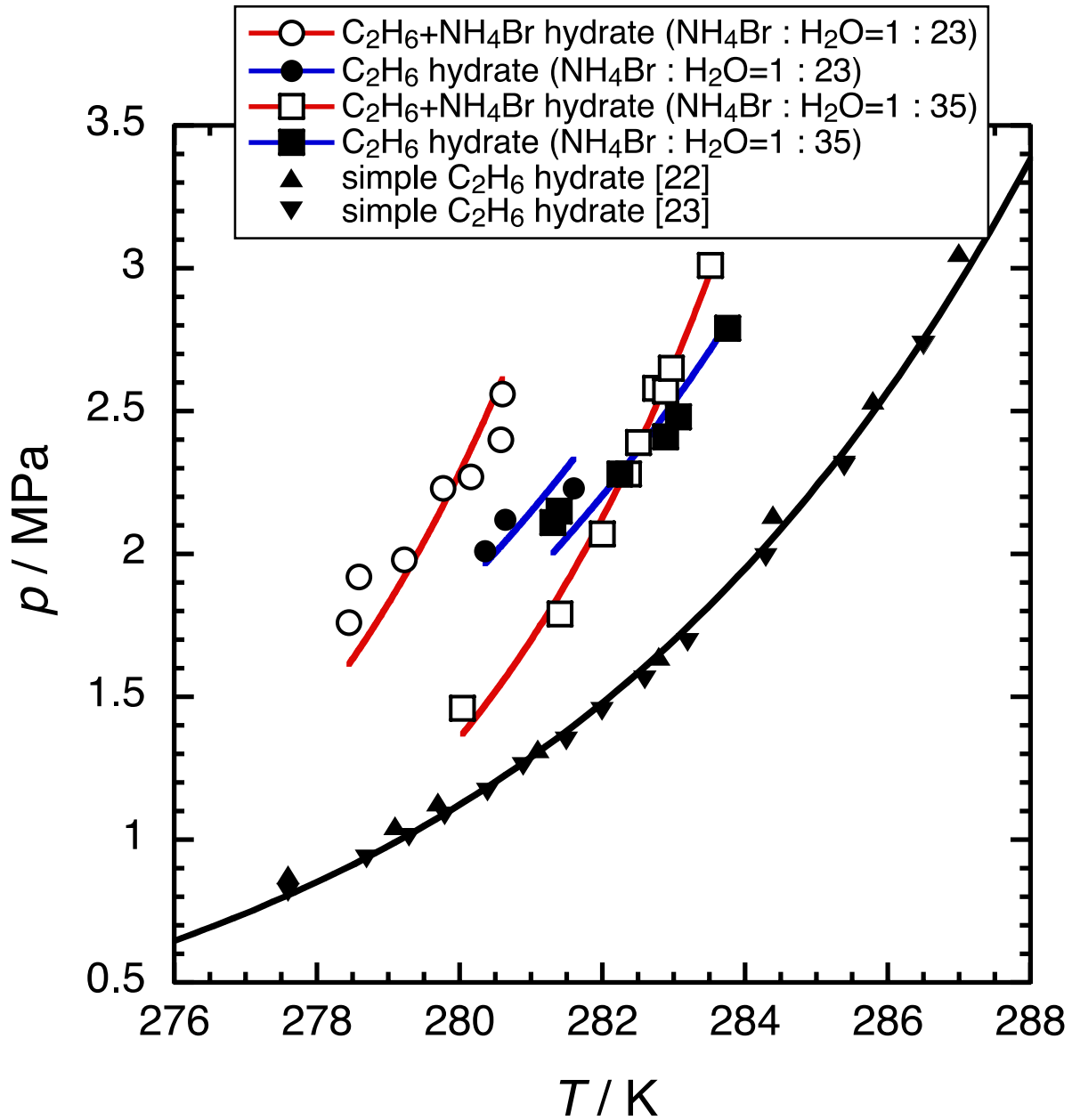system of C_2H_6+water (black curve) [22,23].

Table 1. Phase equilibrium data (m; metastable state) in the ternary system of $C_2H_6+NH_4Br+water$.

T / K	p / MPa	T / K	p / MPa
$NH_4Br : H_2O = 1 : 35$		$NH_4Br : H_2O = 1 : 23$	
($x_{NH4Br} = 0.028$)		($x_{NH4Br} = 0.042$)	
$C_2H_6+NH_4Br$ hydrate		$C_2H_6+NH_4Br$ hydrate	
280.04	1.46	278.45 (m)	1.76 (m)
281.41	1.79	278.59 (m)	1.92 (m)
282.00	2.07	279.23 (m)	1.98 (m)
282.37	2.28	279.77 (m)	2.23 (m)
282.51 (m)	2.39 (m)	280.16 (m)	2.27 (m)
282.75 (m)	2.58 (m)	280.58 (m)	2.40 (m)
282.89 (m)	2.57 (m)	280.60 (m)	2.56 (m)
282.97 (m)	2.65 (m)		
283.52 (m)	3.01 (m)		
sI C_2H_6 hydrate formation		sI C_2H_6 hydrate formation	
281.31 (m)	2.11 (m)	280.36	2.01
281.40 (m)	2.15 (m)	280.64	2.12
282.25 (m)	2.28 (m)	281.60	2.23
282.89	2.41		
283.07	2.48		
283.76	2.79		
structural transition point		expected structural transition point	
282.4±0.1	2.31±0.04	278.5±0.2	1.8±0.1

Table 2. Phase equilibrium data in the ternary system of $C_2H_6+NH_3+$water.

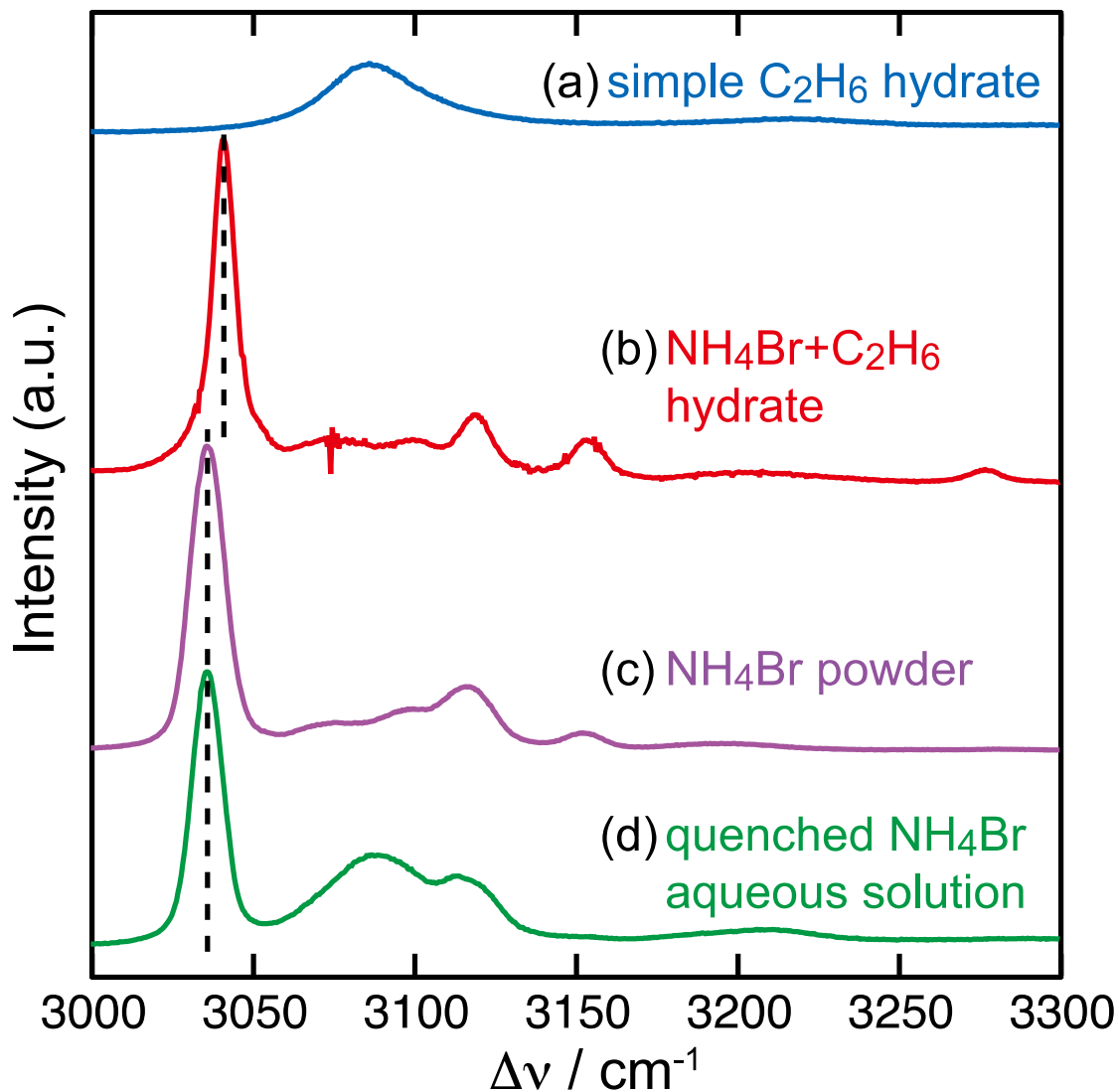| T / K	p / MPa	T / K	p / MPa
$NH_3 : H_2O = 1 : 35$		$NH_3 : H_2O = 1 : 23$	
($x_{NH3} = 0.028$)		($x_{NH3} = 0.042$)	
282.45	1.61	283.30	2.04
284.40	2.16	285.45	2.78
284.54	2.17		
284.90	2.29		
285.32	2.46		
285.56	2.56		
286.93	3.13		
287.31	3.28		

Fig. 1. Three-phase equilibrium curves of hydrate+aqueous+gas phases in the ternary system of C$_2$H$_6$+NH$_4$Br+water and the binary system of C$_2$H$_6$+water [22,23].
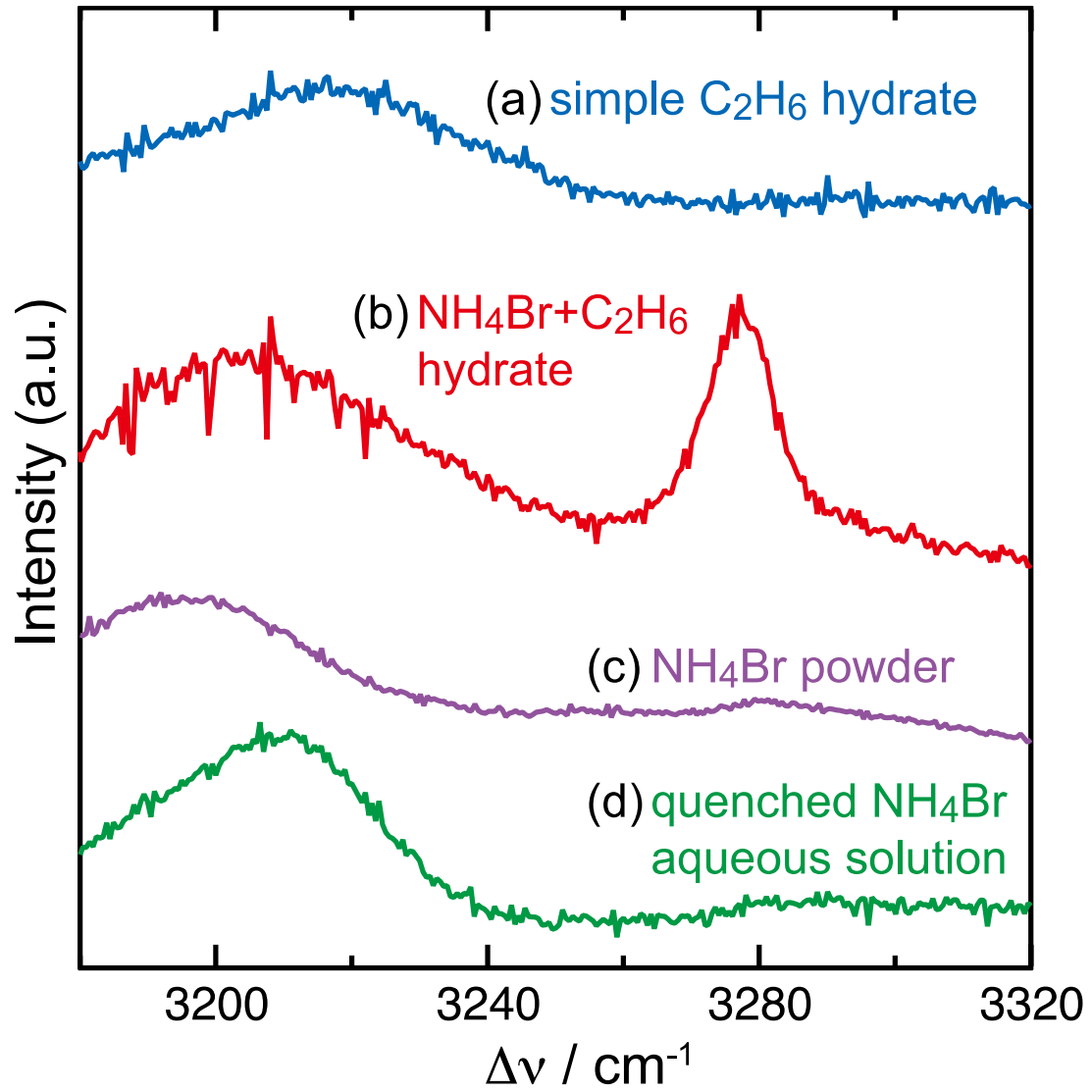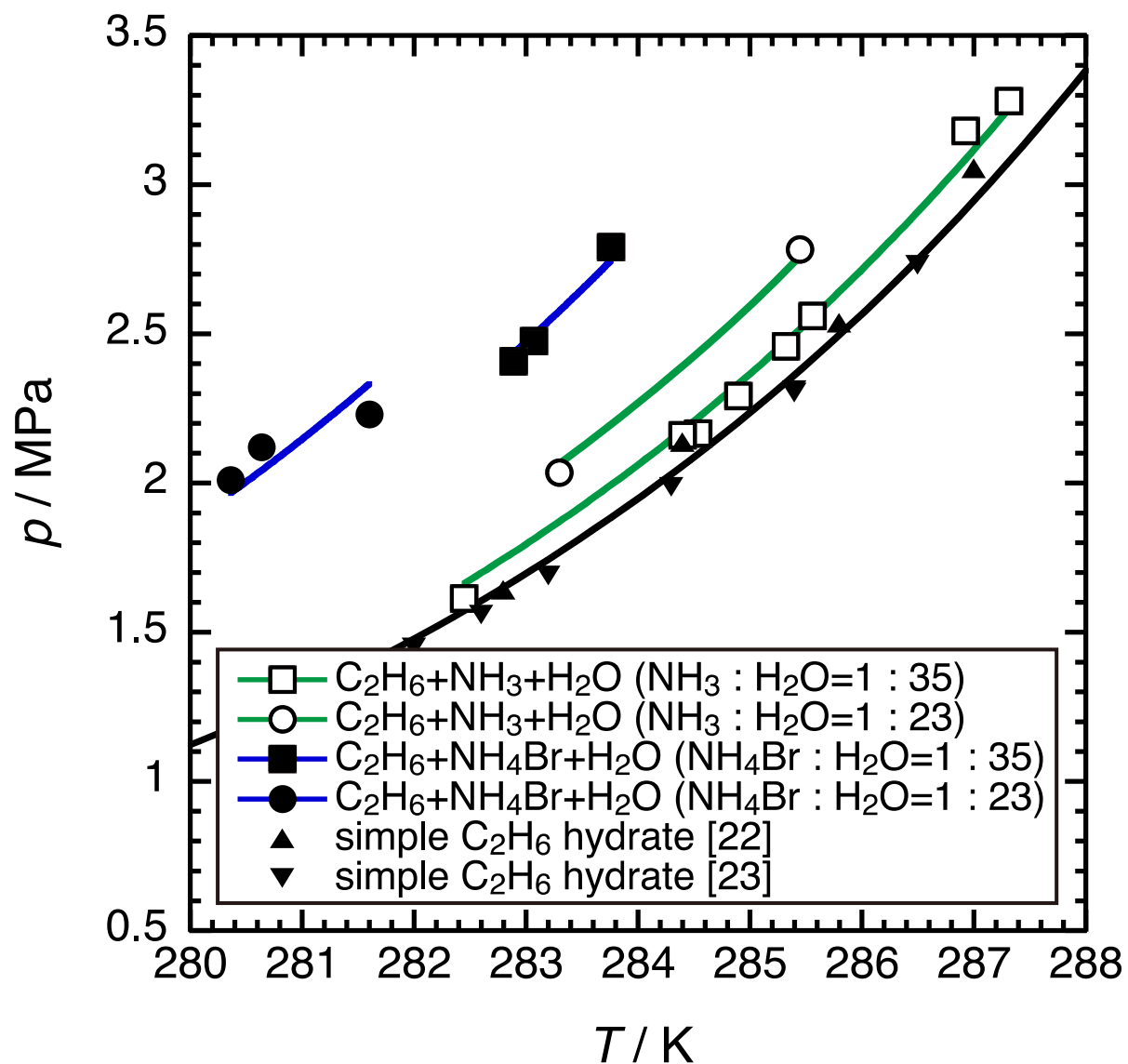
Fig. 2. Raman spectra of the C–C stretching vibration of C_2H_6 molecule in the simple C_2H_6 hydrate (a), $NH_4Br+C_2H_6$ hydrate (b), and solid C_2H_6 (c). All spectra were recorded at 77 K and 0.1 MPa.

Fig. 3. Raman spectra of the N–H stretching vibration of NH_4^+ in $NH_4Br+C_2H_6$ hydrate (b), powder NH_4Br (c), and quenched NH_4Br aqueous solution (d). The spectrum (a) corresponds to the O–H vibration region in the simple C_2H_6 hydrate. All spectra were recorded at 77 K and 0.1 MPa.

Fig. 4. Enlargement around 3280 cm^{-1} in Figure 3.

Fig. 5. Three-phase equilibrium curves of C_2H_6 hydrate+aqueous+gas phases in the ternary systems of C_2H_6+NH_3+water (green curves) and C_2H_6+NH_4Br+water (blue curves) and the binary system of C_2H_6+water (black curve) [22,23].